

Spectroscopic Characterization and Catalytic Application of Copper(I), Silver(I) and Gold(I) Carbonyl Cations in Strong Acids

Nobuko Tsumori,[#] Qiang Xu,[*,#] Mai Hirahara, Souichi Tanihata, Yoshie Souma, Yasuo Nishimura, Nobuhiro Kuriyama, and Susumu Tsubota

National Institute of Advanced Industrial Science and Technology (AIST), 1-8-31 Midorigaoka, Ikeda, Osaka 563-8577

(Received April 5, 2002)

Detailed IR, Raman, and NMR spectroscopic characterization has been carried out on the group 11 metal carbonyl cations, $Cu(CO)_n^+$ (n = 1, 2, 3, 4), $Ag(CO)_n^+$ (n = 1, 2, 3), and $Au(CO)_n^+$ (n = 1, 2), over a wide range of temperature and in a variety of strong acids. Based on these results their molecular structures were determined and their stabilities are compared and discussed. The active species have been determined to be $Cu(CO)_2^+$ (and $Cu(CO)_3^+$ as a minor species) instead of the previously assigned $Cu(CO)_3^+$, $Ag(CO)^+$ instead of the previously assigned $Ag(CO)_2^+$, and $Au(CO)_2^+$, respectively, for the copper(I), silver(I) and gold(I) carbonyl cation-catalyzed carbonylation of olefins and alcohols in concentrated sulfuric acid. The reaction mechanism previously proposed for the metal carbonyl cation-catalyzed carbonylation has been modified to involve an olefin-metal-monocarbonyl (e.g., for Ag) or an olefin-metal-polycarbonyl (e.g., for Cu or Au) intermediate.

Carbon monoxide is one of the most important and versatile ligands in transition metal chemistry.[1] Since the discovery of the first metal carbonyl complexes, $Pt(CO)_2Cl_2$, $Pt_2(CO)_4Cl_4$, and $Pt_2(CO)_3Cl_4$, by Schützenberger in 1868,[2–5] metal carbonyls have played a very important role in chemistry and in the chemical industry.[6,7] Many industrial processes employ CO as a reagent and transition metal compounds as heterogeneous or homogeneous catalysts and involve the intermediates of metal carbonyls.[8–12] The metal-carbonyl bonding has been suggested to involve a synergistic interaction between σ-donor bonding from the occupied 5σ molecular orbital of CO into an empty metal orbital with σ symmetry and π-backbonding from occupied metal orbitals into the π^* molecular orbitals of CO.[1]

Recently, there have been remarkable developments in the synthesis and characterization of new homoleptic metal carbonyl cations and their derivatives from groups 6 through 12 in acidic or superacidic media or with weakly coordinating anions, in which the CO ligand primarily functions as a σ donor.[13–21] Protic acids have been used to generate a number of metal carbonyl cations and cationic carbonyl derivatives as well as molecular adducts of CO to metal cations,[22,23] many of which have been used as catalysts for the carbonylation of olefins and alcohols.[24–35] In strongly acidic solutions, Cu_2O, Ag_2O and Au_2O_3 absorbed carbon monoxide to give colorless, cationic carbonyl complexes of the general formula $[L_mM(CO)_n]^+$ (M = Cu, Ag, Au; L denotes the solvent ligand, probably the conjugate base of the solvent acid or a closely related species), which show high catalytic activities for the carbonylation of olefins and alcohols.[24–29] For the sake of brevity, the solvated cations that should exist in the form of $[L_mM(CO)_n]^+$ will hereafter be simply formulated as $M(CO)_n^+$. The actual stoichiometry of the group 11 metal carbonyl cations depends on the solvent acid and the temperature; so far only limited spectroscopic data have been reported.[24,29,36]

In this paper, we report the detailed spectroscopic characterization of the group 11 metal carbonyl cations over a wide range of temperature and in solvents of various acidities, based on which, their structures have been determined. In addition, discussions are given on the active species and the reaction mechanism of the metal carbonyl cation-catalyzed carbonylation of olefins and alcohols.

Experimental

(a) Chemicals. Cu_2O (Wako Pure Chemical Industries), Ag_2O (Wako Pure Chemical Industries), Au_2O_3 (Rare Metallic Co.), H_2SO_4 (96%, Kanto Chemical Co.), HSO_3F (Wako Pure Chemical Industries), $HSO_3F{\cdot}SbF_5$ (1:1) (Aldrich Chemical Company) and CO (Nippon Sanso) were used. These chemicals were high-purity grade and were used without further purification.

(b) General Procedures. Preparation of the metal carbonyls was performed with a 100-mL three-necked flask connected to a carbon monoxide gas buret. The apparatus containing a mixture of a metal compound (2 mmol, based on the metal atom) and a strong acid (10 mL) was evacuated by a rotary pump to remove air. After carbon monoxide was introduced from the gas buret, the mixture was stirred vigorously until the completion of the reaction. The amount of absorbed CO was measured by the gas buret. In 96% H_2SO_4, HSO_3F or magic acid, $HSO_3F{\cdot}SbF_5$ (1:1), clear solutions were obtained for silver(I) and gold(I) carbonyl cations. Stable heterogeneous suspensions were formed from Cu_2O or Cu under CO atmosphere, which were used as prepared for the spectroscopic measurements. All the manometric and spectroscopic measurements were performed under CO atmosphere unless the spectra for the evacuated samples were obtained under argon atmosphere. For temperature-variable measurements, the sample

Graduate School of Science and Technology, Kobe University, 1-1 Rokkodai-cho, Nada-ku, Kobe, Hyogo 657-8501

was first prepared at room temperature and then cooled or heated to each temperature, where the sample was rigorously stirred under CO atmosphere until reaching the equilibrium.

(c) Instrumentation. In situ FT-IR spectra were recorded using a ReactIR1000 System (ASI, Millersville, MD) with a spectral resolution of 2 cm^{-1} on a zirconia-attenuated total reflection (ATR) sensor (ZirComp) (for Cu and Ag) or a Diamond ATR sensor (DiComp) (for Au).

FT-Raman spectra were recorded on a Nicolet FT-Raman 960 spectrometer with a spectral resolution of 2 cm^{-1} using the 1064 nm exciting line (~600 mV) of a Nd:YAG laser (Spectra Physics, USA). Standard canula transfer techniques were used for the sample manipulations for the room-temperature Raman measurements, for which liquid Raman samples were contained in a 5-mm o.d. NMR tube. For in situ temperature-variable Raman measurements, the liquid samples were contained in a Pyrex tube connected to the three-necked flask and mounted on the cryostat.

^{13}C NMR spectra were recorded using a JEOL JNM-AL400 spectrometer operating at 100.40 MHz. $CDCl_3$ was contained as an external reference and a lock in sample tubes of 5 mm o.d., in which coaxial inserts containing liquid samples were placed. Standard canula transfer techniques were used for the sample manipulations. Carbon monoxide of natural abundance was used for ^{13}C NMR measurements. Chemical shifts are given in δ unit (parts per million) downfield from tetramethylsilane.

Results and Discussion

(a) Copper(I) Carbonyls. A number of copper(I) compounds are reported to absorb carbon monoxide with a CO/Cu stoichiometric ratio $\leq$ 1.0 to form Cu(CO)X under various conditions.[37–43] Souma et al. previously reported the formation of $Cu(CO)_4^+$, $Cu(CO)_3^+$ and $Cu(CO)^+$ from Cu_2O in strong acids such as H_2SO_4, CF_3SO_3H, HSO_3F, HF and $BF_3{\cdot}H_2O$, while $Cu(CO)_2^+$ was not considered.[24] We report here the detailed spectroscopic investigation of this system, which shows the formation of $Cu(CO)_n^+$ (n = 1, 2, 3, 4).

When Cu_2O or Cu reacts with atmospheric CO in 96% H_2SO_4, HSO_3F or magic acid, $HSO_3F{\cdot}SbF_5$ (1:1), a heterogeneous suspension is formed at room temperature; Cu(II) compounds, such as CuO and $CuSO_4$, do not react with CO in these acids. The actual CO/Cu^+ stoichiometry depends on the temperature and the acid solvent. With increasing acidity of the solution or decreasing temperature, the CO/Cu^+ stoichiometry was increased: under atmospheric CO pressure, 1.5 at 23 °C and 2.1 at −10 °C in 96% H_2SO_4; 2.8 at 23 °C and 3.9 at −70 °C in HSO_3F; 3.6 at 23 °C and 3.9 at −40 °C in magic acid, $HSO_3F{\cdot}SbF_5$ (1:1) (Fig. 1). In situ infrared and FT-Raman spectra at varying temperatures exhibit obvious evidence for the formation of the copper(I) carbonyl cations, $Cu(CO)_n^+$ (n = 1, 2, 3, 4), under atmospheric pressure of CO. The equilibra shown in Scheme 1 are shifted to the right as the temperature decreases.

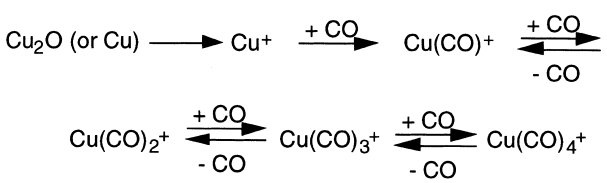

Scheme 1.

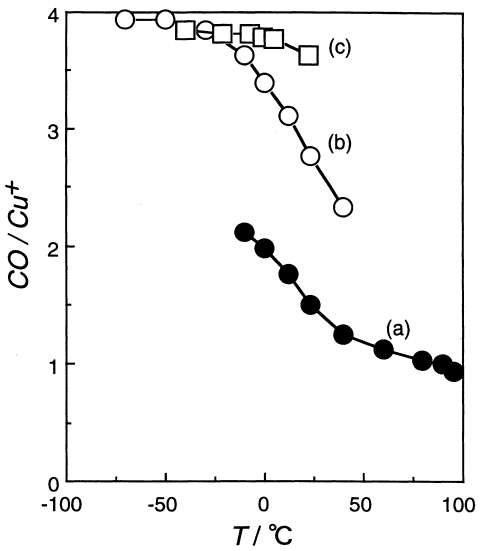

Fig. 1. CO uptake of Cu_2O dissolved in (a) 96% H_2SO_4, (b) HSO_3F, and (c) magic acid, $HSO_3F{\cdot}SbF_5$ (1:1), at varying temperatures under atmospheric pressure of CO.

In 96% H_2SO_4 solution at room temperature, where CO/Cu^+ = 1.5, the IR spectrum exhibits a strong ν(CO) band at 2159 cm^{-1} and a weak IR band at 2187 cm^{-1} (Fig. 2c), and the corresponding Raman spectrum shows a weak band at 2157 cm^{-1} and a strong band at 2189 cm^{-1} (Fig. 3a), which are attributed to $Cu(CO)_2^+$. According to the "mutual exclusive

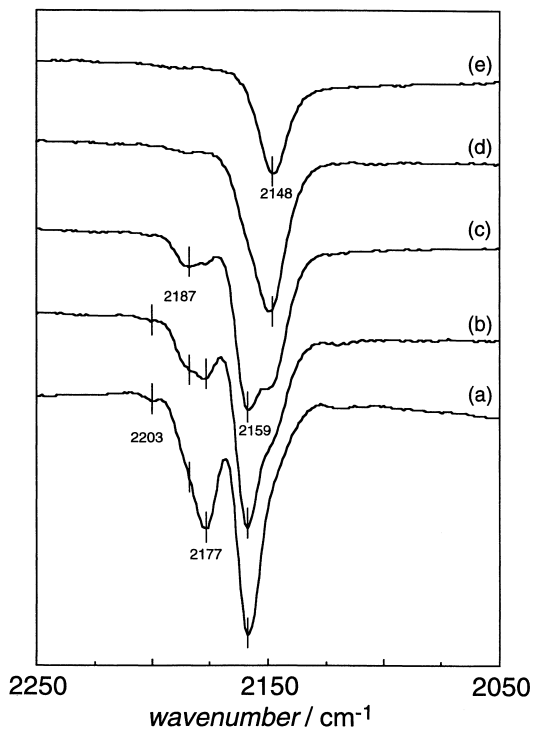

Fig. 2. IR spectra of copper(I) carbonyl cations in 96% H_2SO_4 at (a) −10 °C, (b) 12 °C, (c) 23 °C, and (d) 80 °C under atmospheric pressure of CO, and (e) after evacuating the sample at 23 °C for 10 min.

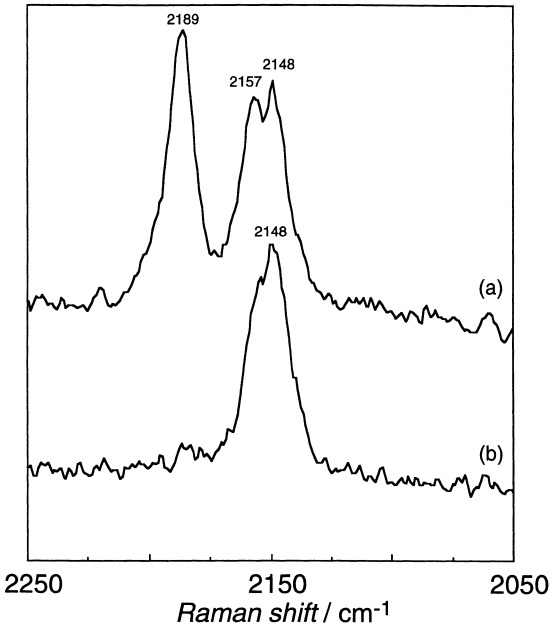

Fig. 3. Raman spectra of copper(I) carbonyl cations in 96% H_2SO_4 (a) at 23 °C under atmospheric pressure of CO, and (b) after evacuating the sample at 23 °C for 10 min.

rule",[44] the IR/Raman coincidences indicate a non-linear symmetry (bent, C_{2v}) for $Cu(CO)_2^+$. The IR bands at the higher frequencies decrease in intensity and the shoulder at 2148 cm^{-1} grows in intensity, accompanied by the CO evolution, with increasing temperature; at 80 °C, the band at 2148 cm^{-1} has the largest intensity (Fig. 2d). In addition, by a brief evacuation of the sample at room temperature, only the IR band at 2148 cm^{-1} (Fig. 2e) along with its corresponding Raman band at the same frequency (Fig. 3b) is left, which is assigned to the copper(I) monocarbonyl cation, $Cu(CO)^+$. At room temperature, a $\nu(CO)_{IR}$ shoulder is observed at 2177 cm^{-1}, which grows, along with the band at 2203 cm^{-1}, with decreasing temperature (Figs. 2a, 2b). These two bands are attributed to $Cu(CO)_3^+$, in which the three CO ligands are out of plane (C_{3v}). Note that in 96% H_2SO_4 solution at room temperature, the copper(I) mono-, di- and tri- carbonyl cations, $Cu(CO)_n^+$ (n = 1, 2, 3), coexist in equilibrium and the dicarbonyl cation, $Cu(CO)_2^+$, rather than $Cu(CO)_3^+$, is the major species, whereas in the previous reports $Cu(CO)_2^+$ was not considered and $Cu(CO)_3^+$ was assigned as the active species for the carbonylation of olefins and alcohols in conc. H_2SO_4 (vide infra).[24,25] At room temperature, only a single resonance appears at 168 ppm in the ^{13}C NMR spectrum, for which a rapid CO exchange on the NMR time scale between the species, $Cu(CO)_n^+$ (n = 1, 2, 3), would account. By removing the ambient CO by evacuation, one finds that the solution gives a single peak at 166 ppm, which is attributed to $Cu(CO)^+$.

In HSO_3F at room temperature, where $CO/Cu^+ = 2.8$, the IR spectrum exhibits a strong $\nu(CO)$ band at 2184 cm^{-1} and a shoulder at 2207 cm^{-1} (Fig. 4c). The corresponding Raman spectrum shows a weak band at 2185 cm^{-1} and a strong band at 2209 cm^{-1} (Fig. 5a). These bands can be attributed to $Cu(CO)_3^+$ that has a structure (C_{3v}) with an out-of-plane deviation from a trigonal plane (D_{3h}). The Raman band at 2209 cm^{-1} is strongly polarized (Figs. 5a, 5b); along with its IR counterpart at 2207 cm^{-1}, it is assigned to the symmetric CO stretch. The Raman band at 2185 cm^{-1} is depolarized; along with its

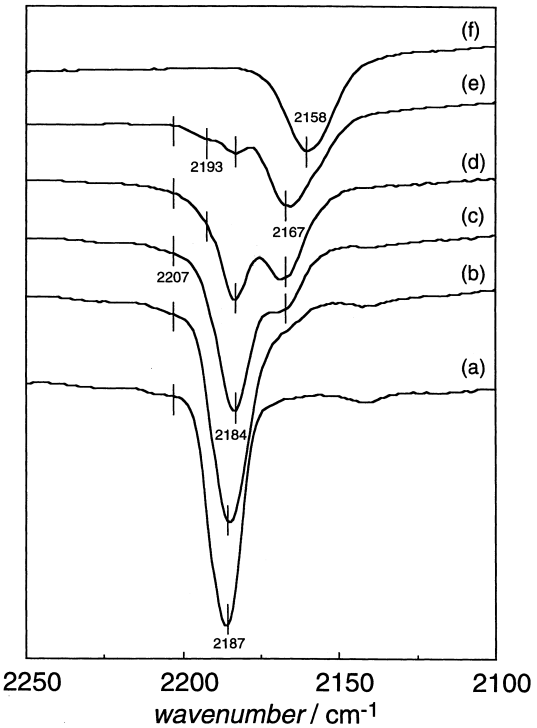

Fig. 4. IR spectra of copper(I) carbonyl cations in HSO_3F at (a) −70 °C, (b) 0 °C, (c) 24 °C and (d) 40 °C under atmospheric pressure of CO, and after evacuating the sample at 24 °C (e) for 5 sec and (f) for 10 min.

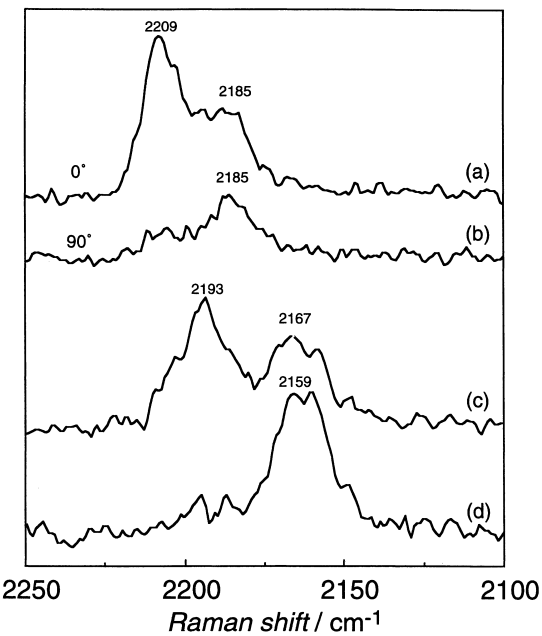

Fig. 5. Raman spectra of copper(I) carbonyl cations in HSO_3F with (a) 0° and (b) 90° polarization filters at 24 °C under atmospheric pressure of CO, and after evacuating the sample at 24 °C (c) for 5 sec and (d) for 10 min.

IR counterpart at 2184 cm^{-1}, it is assigned to the asymmetric CO stretch. The IR band at 2184 cm^{-1} due to $Cu(CO)_3^+$ slightly shifts to 2187 cm^{-1} on decreasing the temperature from 24 to −70 °C (Figs. 4c–4a). However, for $CO/Cu^+ = 3.9$ at −70 °C, no IR band due to $Cu(CO)_4^+$ was observed, due to its low solubility, as also observed in magic acid (vide infra). If one raises the temperature from room temperature, the IR bands at higher frequencies decrease in intensity and the shoulder at 2167 cm^{-1} grows in intensity, accompanied by CO evolution (Figs. 4c, 4d). At 40 °C where the CO/Cu^+ ratio is 2.3, the IR band at 2167 cm^{-1} with an intensity comparable to that at 2184 cm^{-1} and a shoulder at 2193 cm^{-1} are observed (Fig. 4d). In addition, by a brief evacuation for 5 sec at room temperature, the IR band at 2184 cm^{-1} is remarkably decreased and the IR bands at 2167 and 2193 cm^{-1} are enhanced (Fig. 4e); the corresponding Raman spectrum shows a band at 2167 cm^{-1} and a band at 2193 cm^{-1} with a larger intensity (Fig. 5c); these are attributed to $Cu(CO)_2^+$ with a non-linear structure (bent, C_{2v}). Upon an evacuation for 10 min at room temperature, the high-frequency bands disappear and a new IR band at 2158 cm^{-1} (Fig. 4f) with the corresponding Raman band at 2159 cm^{-1} (Fig. 5d) appears, which can be assigned to $Cu(CO)^+$. It is noted that in HSO_3F, the copper(I) mono-, di- and tri- carbonyl cations, $Cu(CO)_n^+$ (n = 1, 2, 3), coexist in equilibrium and the tricarbonyl cation, $Cu(CO)_3^+$, is the major species at room temperature. At room temperature, only a single resonance appears at 169 ppm in the ^{13}C NMR spectrum, for which the rapid CO exchange on the NMR time scale between the species, $Cu(CO)_n^+$ (n = 1, 2, 3), would account. By removing the ambient CO by evacuation, one finds that the solution gives a single peak at 166 ppm due to the stable $Cu(CO)^+$.

In magic acid, $HSO_3F{\cdot}SbF_5$ (1:1), at atmospheric pressure of CO and room temperature, a white suspension is formed with $CO/Cu^+ = 3.6$. A ν(CO) band at 2190 cm^{-1} in the IR spectrum (Fig. 6a), two strong bands at 2187 and 2211 cm^{-1} and a shoulder at 2192 cm^{-1} in the Raman spectrum (Fig. 7b) were observed. The IR band at 2190 cm^{-1} decreases in intensity with decreasing temperature; at −40 °C, it mostly disappears (Figs. 6a–6d). We assign the IR band at 2190 cm^{-1} along with the corresponding Raman bands at 2192 and 2211 cm^{-1} to $Cu(CO)_3^+$. The lack of an IR counterpart of the Raman band at 2211 cm^{-1} indicates that $Cu(CO)_3^+$ has an almost trigonal-planar (D_{3h}) structure, in contrast with the out-of-plane structure for $Cu(CO)_3^+$ in conc. H_2SO_4 or HSO_3F, probably owing to the lower nucleophilicity of magic acid. The Raman band at 2187 cm^{-1} is assigned to $Cu(CO)_4^+$, even though we could detect only one Raman band instead of the two predicted for $Cu(CO)_4^+$ with tetrahedral geometry (T_d). The Raman band at 2187 cm^{-1} grows in intensity with decreasing temperature and therefore increasing concentration of $Cu(CO)_4^+$ (Fig. 7a). The lack of an IR ν(CO) band corresponding to the Raman band at 2187 cm^{-1} for $Cu(CO)_4^+$ is probably due to its low solubility, because the attenuated total reflection (ATR) IR sensor can detect only soluble species, while both soluble and insoluble species can be detected in the Raman measurements. This assignment is supported by the examination conducted with evacuation of the solution. After only a brief evacuation (5 min) at −20 °C, the white solids in the suspension immediately disappear, giving a clear and colorless solution. The IR band at 2190 cm^{-1} increases in intensi-

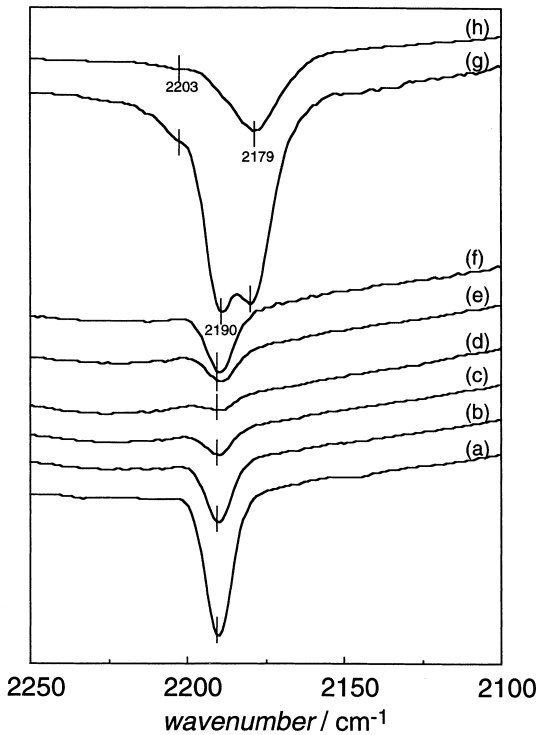

Fig. 6. IR spectra of copper(I) carbonyl cations in magic acid, $HSO_3F{\cdot}SbF_5$ (1:1), at (a) 23 °C, (b) 0 °C, (c) −20 °C and (d) −40 °C under atmospheric pressure of CO, and after evacuating the sample at −20 °C (e) for 5 min and (f) for 3 h, and after evacuating the sample at 23 °C (g) for 2 h and (h) for 6 h.

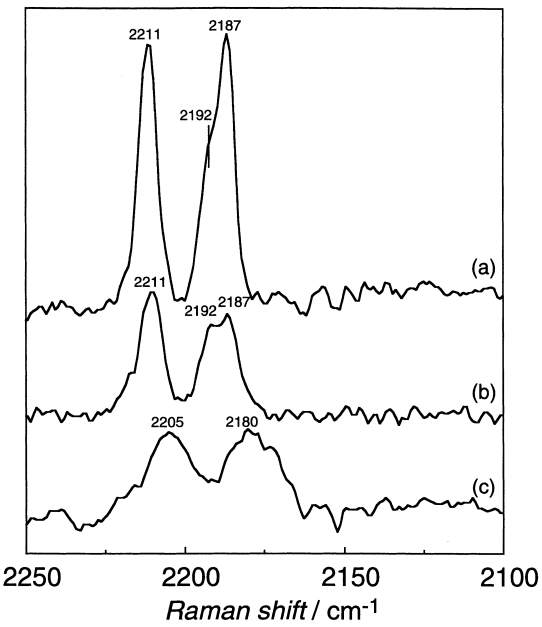

Fig. 7. Raman spectra of copper(I) carbonyl cations in magic acid, $HSO_3F{\cdot}SbF_5$ (1:1), at (a) −20 °C, (b) 23 °C, and (c) after evacuating the sample at 23 °C for 6 h.

ty due to the evacuation (Figs. 6e, 6f). We believe that $Cu(CO)_4^+$, the white solids in the suspension, undetectable by the ATR IR sensor, readily release one CO ligand by evacuation to form $Cu(CO)_3^+$, which is soluble and detectable by the ATR IR sensor. At room temperature, no ^{13}C NMR signal was detected from the clear solution obtained by decanting the suspension from the solution prepared with CO of natural abundance, because most of the Cu^+ has been precipitated as $Cu(CO)_4^+$ so that the concentration of $Cu(CO)_3^+$ in the solution is too low to be detected. After a brief evacuation for 30 s at room temperature, the white solids in the suspension quickly disappear, giving a colorless, clear solution which exhibits a ^{13}C NMR resonance at 169 ppm due to $Cu(CO)_3^+$. Further prolonged evacuation of the solution leads to the loss of one CO ligand from $Cu(CO)_3^+$ to form $Cu(CO)_2^+$, which has a non-linear structure (bent, C_{2v}); two IR bands at 2179 (strong) and 2203 (weak) cm^{-1} (Figs. 6g, 6h) and two corresponding Raman bands at 2180 and 2205 cm^{-1} (Fig. 7c) were observed, as observed in conc. H_2SO_4 and HSO_3F. $Cu(CO)_2^+$ in magic acid exhibits a ^{13}C NMR resonance at 166 ppm.

All the IR and Raman ν(CO) values observed for $Cu(CO)_n^+$ (n = 1–4) are higher than 2143 cm^{-1}, the value for free CO,[44] indicating reduced π-backbonding, as observed for a series of metal carbonyl cations, whereas typical metal carbonyls exhibit much lower ν(CO) values.[16] The ^{13}C NMR chemical shifts shown by the copper(I) carbonyl cations are high field-shifted from 184 ppm, the value for free CO,[45] as observed for a series of metal carbonyl cations, whereas a low-field shift from 184 ppm is usually observed for typical metal carbonyls.[16] It is noted that $Cu(CO)_2^+$ is bent (C_{2v}) in all these acids whereas $Cu(CO)_3^+$ is non-planar (C_{3v}) in conc. H_2SO_4 and HSO_3F but almostly trigonal planar (D_{3h}) in magic acid. Therefore, in a solution that is sufficiently nucleophilic, Cu^+ tends to assume a tetrahedral coordination geometry, in which the coordination sites unoccupied by CO ligands are occupied by the solvent molecules. By comparison, the two-coordinate, linear structure ($D_{\infty h}$) for $Cu(CO)_2^+$ and the three-coordinate, trigonal-planar structure (D_{3h}) for $Cu(CO)_3^+$ are observed in solid $[Cu(CO)_n][AsF_6]$ (n = 2, 3)[46] and in the rare-gas matrices,[47] but the bent $Cu(CO)_2^+$ and non-planar $Cu(CO)_3^+$ are observed in zeolites[48–50] and in $Cu(CO)_n(N(SO_2CF_3)_2)$ (n = 2, 3)[51] (Fig. 8). The copper(I) tetracarbonyl cation, $Cu(CO)_4^+$, may be tetrahedral (T_d), as observed for solid $[Cu(CO)_4][1\text{-Et-}CB_{11}F_{11}]$[52] or the isoelectronic $Ni(CO)_4$, $Co(CO)_4^-$ and $Fe(CO)_4^{2-}$.[53]

It seems that the stability of the copper(I) carbonyls increases with increasing acidity of the solvent acid. The monocarbonyl $Cu(CO)^+$ is stabler than $Cu(CO)_2^+$ and $Cu(CO)_3^+$ in concentrated H_2SO_4 solution; the unstable polycarbonyls readily release CO ligands to form $Cu(CO)^+$ upon brief evacuation, but $Cu(CO)^+$ survives even after continuous evacuation over 24 hours. Also in HSO_3F, only $Cu(CO)^+$ survives upon evacuation, but in magic acid, $Cu(CO)_2^+$ remains unchanged after prolonged evacuation. Note that the lower stability was observed in the solid than in solution as the solid $[Cu(CO)][AsF_6]$ releases CO to form $CuAsF_6$ at 0 torr CO,[46] although $[AsF_6]^-$ is less nucleophilic than the above acid solutions.

(b) Silver(I) Carbonyls. Manchot et al. first reported in the 1920's that Ag_2SO_4 reversibly absorbed CO in concentrated H_2SO_4.[22,23] A CO/Ag stoichiometric ratio of 0.5 was

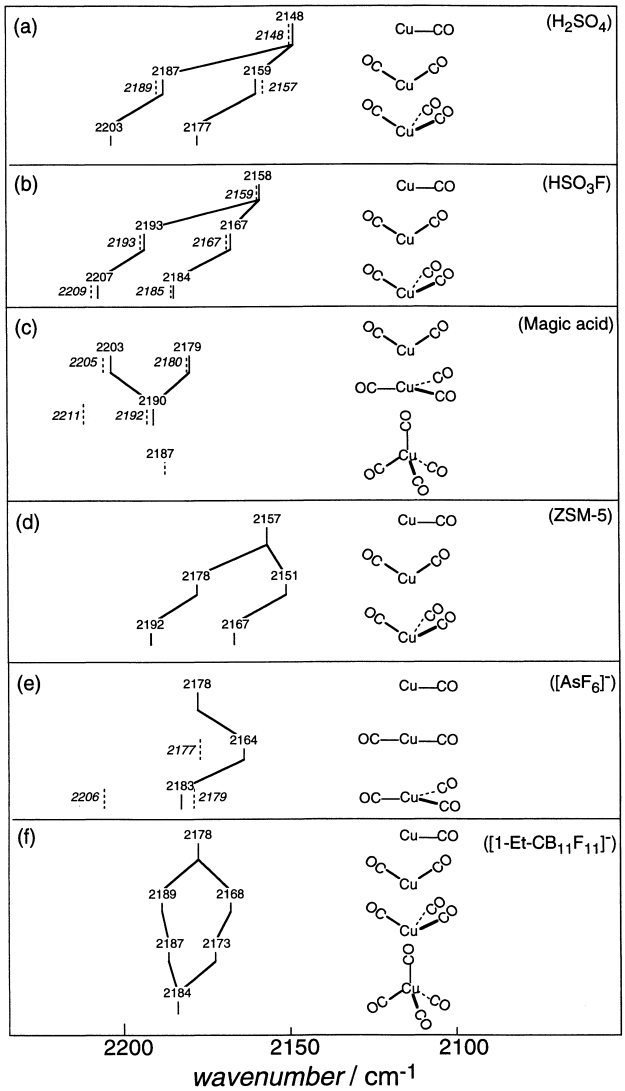

Fig. 8. Schematic representations of $Cu(CO)_n^+$ (n = 1–4) species and corresponding CO vibrational frequncies in (a) 96% H_2SO_4, (b) HSO_3F, (c) magic acid, $HSO_3F{\cdot}SbF_5$ (1:1), (d) the ZSM-5 zeolite, (e) the salt of $[AsF_6]^-$, and (f) the salt of $[1\text{-Et-}CB_{11}F_{11}]^-$. Full and dashed segments represent IR and Raman data, respectively.

achieved at 0 °C and 1 atm of CO. Souma et al. reported that Ag_2O in neat HSO_3F, $BF_3{\cdot}H_2O$ and other strong acids absorbed up to 2 equivalents CO per equivalent Ag, the exact stoichiometry being dependent on temperature and pressure; only the dicarbonyl $Ag(CO)_2^+$ was considered in the strong acids, which was assigned as the active species for the carbonylation of olefins, alcohols and saturated hydrocarbons.[24,54] Strauss and co-workers have isolated the $Ag(CO)^+$ and $Ag(CO)_2^+$ cations by the direct but reversible CO addition to the silver(I) salts of $[B(OTeF_5)_4]^-$, $[Zn(OTeF_5)_4]^{2-}$, $[Nb(OTeF_5)_6]^-$, and $[Ti(OTeF_5)_6]^{2-}$ under different CO pressures; single-crystals of $[Ag(CO)][B(OTeF_5)_4]$ and $[Ag(CO)_2][B(OTeF_5)_4]$ were obtained from the very weakly coordinating solvent 1,1,2-$C_2Cl_3F_3$. Their low temperature X-ray diffraction studies revealed nearly linear Ag–C–O arrays in both of the salts and a linear structure for $[Ag(CO)_2][B(OTeF_5)_4]$.[55–57] Furthermore,

the direct but reversible CO addition to metal salts with weakly coordinating anions at high pressures of CO results in the formation of $[Ag(CO)_3][Nb(OTeF_5)_6]$.[58] Very recently, Willner and co-workers reported that the anion $[B(CF_3)_4]^-$ is very weakly coordinating, as demonstrated by the low equilibrium CO pressure over the $[Ag(CO)_n][B(CF_3)_4]$ (n = 1, 2) salts and the formation of $[Ag(CO)_n][B(CF_3)_4]$ (n = 3, 4) at higher CO pressures.[59] Here we report detailed spectroscopic investigations of the silver(I) carbonyl cations in a variety of strongly acidic solutions and show that in 96% H_2SO_4 only the monocarbonyl cation, $Ag(CO)^+$, is formed and in HSO_3F or magic acid the tricarbonyl complex, $Ag(CO)_3^+$, is formed in addition to $Ag(CO)_n^+$ (n = 1, 2) at atmospheric pressure of CO.

Colorless solutions were obtained when Ag_2O was dissolved in 96% H_2SO_4, HSO_3F and magic acid, $HSO_3F{\cdot}SbF_5$ (1:1), under atmospheric pressure of CO. As shown in Fig. 9, with increasing acidity of the solution or decreasing temperature, the CO/Ag stoichiometry is increased: 0.21 at 22 °C and 0.62 at −10 °C in 96% H_2SO_4; 0.59 at 22 °C and 2.3 at −70 °C in HSO_3F; 2.1 at 22 °C and 2.5 at −30 °C in magic acid. It is noted that the CO/Ag stoichiometry is higher than 2.0, meaning that $Ag(CO)_3^+$ may be formed, in HSO_3F and magic acid at low temperatures under atmospheric pressure of CO. In situ infrared spectra at varying temperatures exhibit obvious evidence for the formation of the silver(I) carbonyl cations, $Ag(CO)_n^+$ (n = 1, 2, 3), under atmospheric pressure of CO (vide infra). The binding of CO to Ag^+ in these acids is reversible, as observed in the solids or a 1,1,2-$C_2Cl_3F_3$ solution of $AgNb(OTeF_5)_6$.[57] The equilibra shown in Scheme 2 are shifted to the right as the temperature decreases.

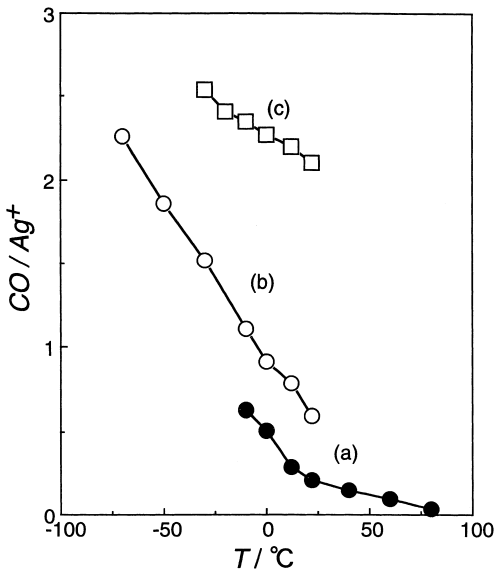

Fig. 9. CO uptake of Ag_2O dissolved in (a) 96% H_2SO_4, (b) HSO_3F and (c) magic acid, $HSO_3F{\cdot}SbF_5$ (1:1), at varying temperatures under atmospheric pressure of CO.

In 96% H_2SO_4 solution, a ν(CO) band was observed at 2186 cm^{-1} in the IR spectrum at room temperature, which grows in intensity at the same frequency with decreasing temperature and decreases in intensity with increasing temperature (Fig. 10). The corresponding Raman band is observed at 2186 cm^{-1} (Fig. 11a), which should be attributed to the silver(I) monocarbonyl cation, $Ag(CO)^+$. Note that no $Ag(CO)_2^+$ species is formed in the 96% H_2SO_4 solution. Similarly to the case in solid salts with weakly coordinating anions,[55–57] $Ag(CO)^+$ is unstable, in contrast with the high stability of $Cu(CO)^+$ in strong acids; the CO ligand is readily removed under vacuum at −10 °C.

In HSO_3F, a ν(CO) IR band at 2190 cm^{-1} (Fig. 12a) with the corresponding Raman band at 2189 cm^{-1} (Fig. 11b) was observed for $Ag(CO)^+$ at room temperature. The IR band first shifts to higher energy with the convolution of the ν(CO) bands for $Ag(CO)^+$ and $Ag(CO)_2^+$ until the temperature is decreased to −60 °C where a ν(CO) band was observed at 2192 cm^{-1} for $Ag(CO)_2^+$ (Fig. 12b, 12c). At −60 °C, the ν(CO) band begins to shift to lower energy with decreasing temperature and reaches 2190 cm^{-1} at −80 °C (Fig. 12d, 12e). Our interpretation is that $Ag(CO)_3^+$, which exhibits a ν(CO) band lower than that for $Ag(CO)_2^+$ (2192 cm^{-1}), is formed below −60 °C, consistent with the CO uptake (Fig. 9b). At −80 °C, the band at 2190 cm^{-1} shifts to 2192 cm^{-1} with a brief evacuation (Fig. 12f), reflecting that one CO ligand can be readily removed from $Ag(CO)_3^+$ to form $Ag(CO)_2^+$, but the latter remains unchanged even after evacuation for 3 h.

Figure 13 shows IR spectra of silver(I) carbonyl cations in magic acid, $HSO_3F{\cdot}SbF_5$ (1:1), under atmospheric pressure of CO at temperatures that range from room temperature to −40 °C. At room temperature, a ν(CO) band was observed at 2203 cm^{-1} (Fig. 13a), and a strongly polarized Raman band was observed at 2210 cm^{-1} (Fig. 11c). This IR band is attributed to the asymmetric CO stretch (Σ_u^+ normal mode) and the Raman band to the symmetric CO stretch (Σ_g^+ normal mode) of the silver(I) dicarbonyl cation, $Ag(CO)_2^+$, which should have a linear structure ($D_{\infty h}$), as observed for solid $[Ag(CO)_2][B(OTeF_5)_4]$.[57] Note that the bent OC–Ag–CO species (C_{2v}) has been observed in zeolites.[60] One CO ligand is readily removed to form $Ag(CO)^+$ (2198 cm^{-1}) under vacuum (Fig. 13e), but a small amount of $Ag(CO)^+$ remains after an evacuation for 1 h at room temperature (Fig. 13f). With decreasing temperature, the IR absorption at 2203 cm^{-1} decreases, and a separate and distinct ν(CO) band, which is assigned to $Ag(CO)_3^+$, grows in intensity at 2196 cm^{-1} (Figs. 13b, 13c). At −40 °C, one CO ligand is readily removed from $Ag(CO)_3^+$ by brief evacuation to form $Ag(CO)_2^+$ (Fig. 13d), but $Ag(CO)_2^+$ survives even after an evacuation for 3 h. Almost the same results were obtained for AgF dissolved in magic ac-

$$Ag_2O \longrightarrow Ag^+ \underset{-CO}{\overset{+CO}{\rightleftharpoons}} Ag(CO)^+ \underset{-CO}{\overset{+CO}{\rightleftharpoons}} Ag(CO)_2^+ \underset{-CO}{\overset{+CO}{\rightleftharpoons}} Ag(CO)_3^+$$

Scheme 2.

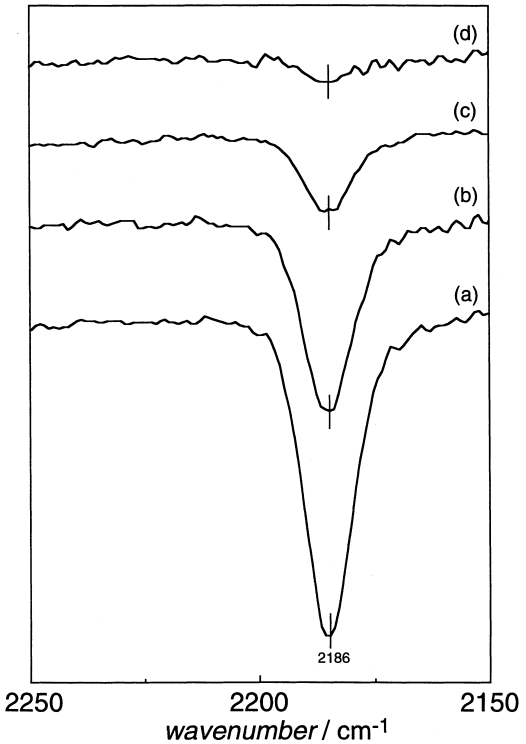

Fig. 10. IR spectra of $Ag(CO)^+$ in 96% H_2SO_4 at (a) −10 °C, (b) 12 °C, (c) 25 °C, and (d) 80 °C under atmospheric pressure of CO.

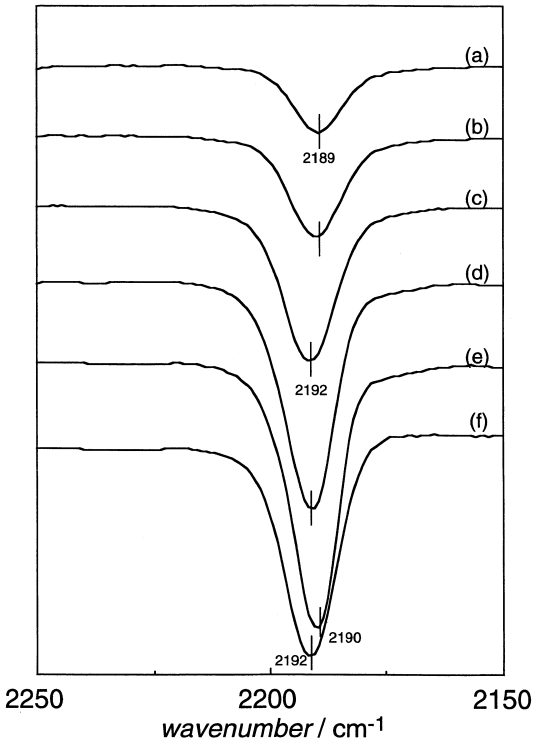

Fig. 12. IR spectra of silver(I) carbonyl cations in HSO_3F at (a) 23 °C, (b) 0 °C, (c) −60 °C, (d) −70 °C, (e) −80 °C and (f) after evacuating the sample at −80 °C for 3 h.

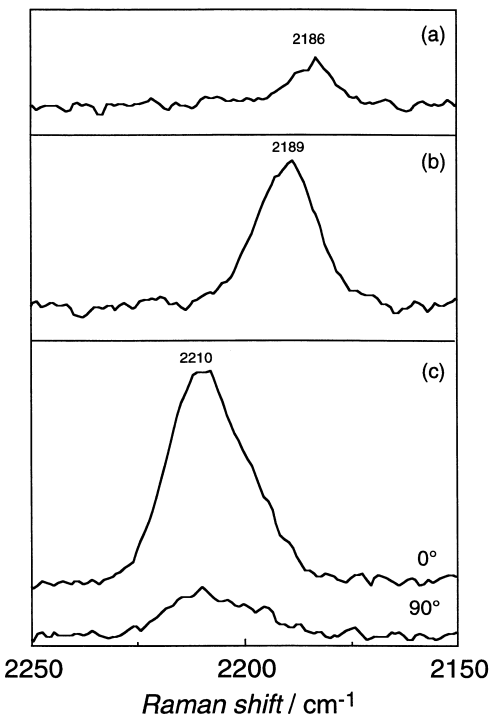

Fig. 11. Raman spectra of silver(I) carbonyl cations in (a) 96% H_2SO_4, (b) HSO_3F, and (c) magic acid, $HSO_3F{\cdot}SbF_5$ (1:1), (upper with 0° polarization filter and bottom with 90° polarization filter) at room temperature under atmospheric pressure of CO.

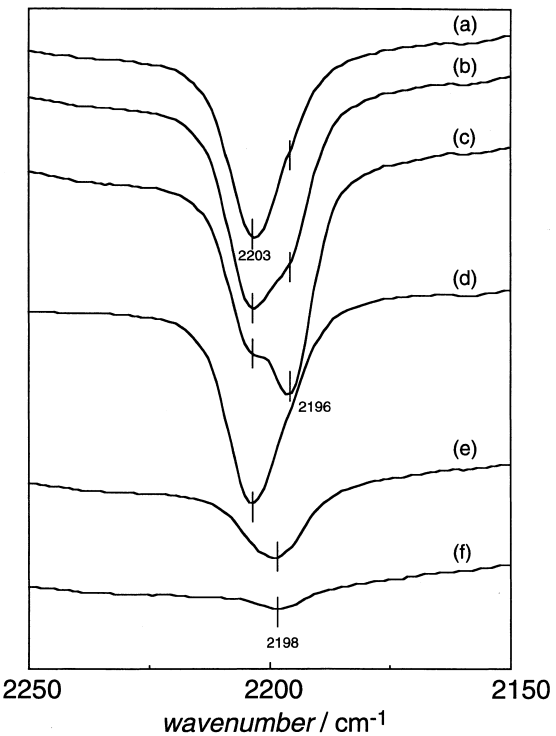

Fig. 13. IR spectra of silver(I) carbonyl cations in magic acid, $HSO_3F{\cdot}SbF_5$ (1:1), at (a) 21 °C, (b) −20 °C and (c) −40 °C under atmospheric pressure of CO, (d) after evacuating the sample at −40 °C for 15 min, and after evacuating the sample at 21 °C (e) for 15 min and (f) for 1 h.

id.

All the IR and Raman ν(CO) values observed for $Ag(CO)_n^+$ (n = 1–3) are higher than 2143 cm^{-1}, the value for free CO. The ^{13}C NMR chemical shifts shown by the silver(I) carbonyl cations are high-field-shifted from 184 ppm, the value for free CO. Single ν(CO) IR bands are observed for each complex, suggesting a linear structure ($D_{\infty h}$) for $Ag(CO)_2^+$ (Σ_u^+ normal mode) and a three-coordinate, trigonal-planar structure (D_{3h}) for $Ag(CO)_3^+$ (E' normal mode), as observed in $[Ag(CO)_n][Nb(OTeF_5)_6]$ (n = 1–3),[55–58] and in rare-gas matrices[61] (Fig. 14). Only for $Ag(CO)_2^+$ in zeolites is the bent structure (C_{2v}) observed.[60] It appears that, in HSO_3F or magic acid, the stability of the complexes is in the order of $Ag(CO)^+ > Ag(CO)_2^+ > Ag(CO)_3^+$, whereas a theoretical calculation (MP2 level) predicted that $Ag(CO)_2^+$ is the stablest.[62] With decreasing acidity of the solution, the ν(CO) bands for each of the silver(I) carbonyl cations shift to low energy. In HSO_3F or magic acid, the ν(CO) bands are in the order of $Ag(CO)_2^+ > Ag(CO)^+ > Ag(CO)_3^+$. In contrast, the ν(CO) bands for $[Ag(CO)_n][Nb(OTeF_5)_6]$ are 2208, 2198, and 2192 for n = 1, 2 and 3, respectively, in the order of $Ag(CO)^+ > Ag(CO)_2^+ > Ag(CO)_3^+$.[55–58] The effects from the solvents (although probably being very weakly coordinating) seem to be important with respect to the observations. Armentrout et al. have reported metal carbonyl bond energies for the gas phase complex ions $Ag(CO)_n^+$ (n = 1-4): $(CO)_xAg^+$–CO bond energies at 0 K were found to be 21(1), 26(1), 13(2) and 11(4) kcal mol^{-1} for x = 0, 1, 2 and 3, respectively.[63] This finding predicts that the bond energy for $Ag(CO)_4^+$ may be close to that for $Ag(CO)_3^+$, which has been recently verified by the formation of $[Ag(CO)_n][B(CF_3)_4]$ (n = 3, 4) at higher CO pressure.[59]

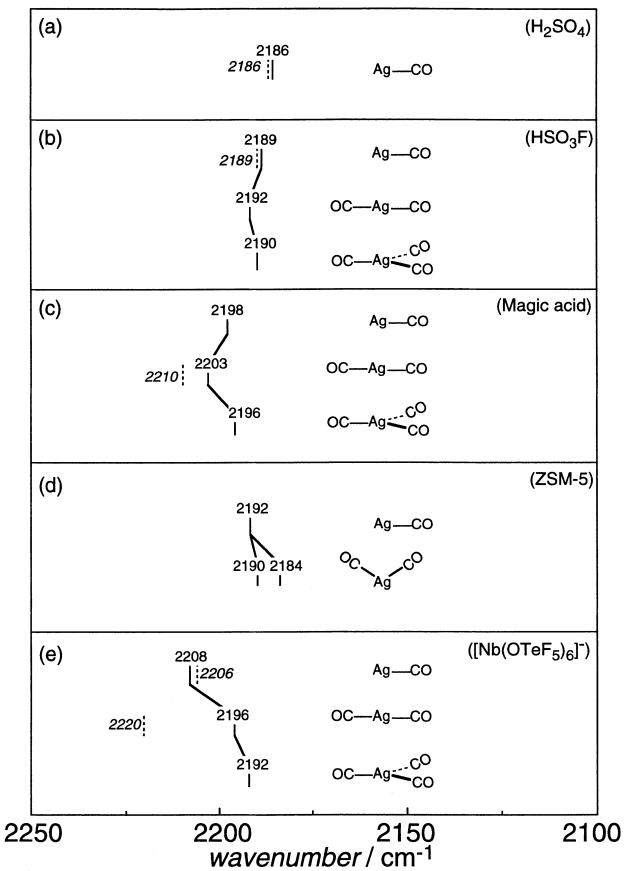

Fig. 14. Schematic representations of $Ag(CO)_n^+$ (n = 1–3) species and corresponding CO vibrational frequencies in (a) 96% H_2SO_4, (b) HSO_3F, (c) magic acid, $HSO_3F{\cdot}SbF_5$ (1:1), (d) the ZSM-5 zeolite, and (e) the salt of $[Nb(OTeF_5)_6]^-$. Full and dashed segments represent IR and Raman data, respectively.

(c) Gold(I) Carbonyls. Only a small number of carbonyl derivatives of gold have been synthesized to date. For more than 65 years, the only isolable gold(I) carbonyl was Au(CO)Cl, first prepared by Manchot and Gall in 1925.[64] Willner et al. reported the isolation of the gold(I) carbonyl cation, $Au(CO)_2^+$, using Lewis superacidic media such as SbF_5; its discovery resulted as an accident from the attempts to prepare the $[HCO]^+$ ion by protonation of CO in the conjugated superacid HSO_3F-$Au(SO_3F)_3$.[65,66] Strauss and co-workers determined that a new IR band at 2212 cm^{-1}, assigned to $[Au(CO)_3][Sb_2F_{11}]$, appears when the dicarbonyl complex, $[Au(CO)_2][Sb_2F_{11}]$, is exposed to 100 atm CO pressure.[67]

We found a facile synthetic method for gold(I) carbonyls suitable for the catalytic carbonylation of olefins and alcohols; the direct reductive carbonylation of gold(III) oxide, Au_2O_3, with CO leads to the formation of $Au(CO)_n^+$ (n = 1, 2).[29] Alternative routes to the formation of the gold(I) carbonyl cations in H_2SO_4 are the oxidation carbonylation of metallic gold with SO_3 as an oxidizing agent and the solvolysis and carbonylation of AuOH. As shown in Fig. 15a, with decreasing temperature, the CO/Au stoichiometry is increased: 1.7 at 23 °C and 2.0 at

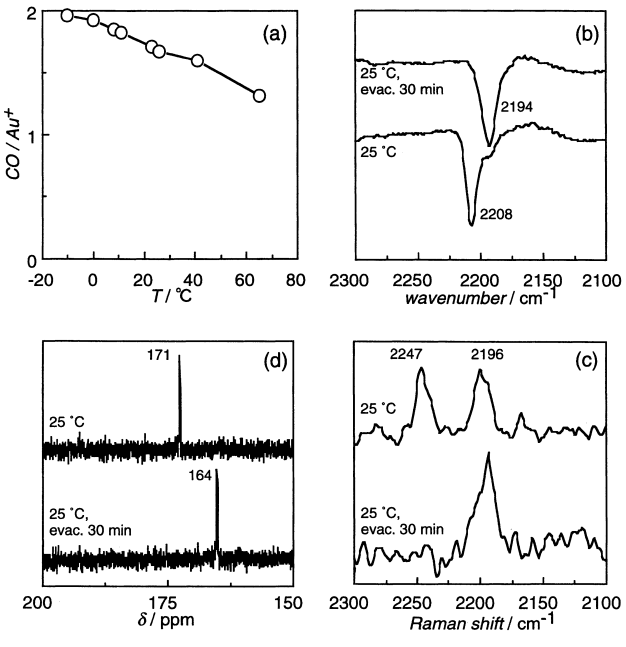

Fig. 15. (a) CO uptake of Au_2O_3, and (b, bottom) IR, (c, upper) Raman, and (d, upper) ^{13}C NMR spectra of $Au(CO)_n^+$ (n = 1, 2) in 96% H_2SO_4 at room temperature under atmospheric pressure of CO (natural abundance), and (b, upper) IR, (c, bottom) Raman, and (d, bottom) ^{13}C NMR spectra after evacuating the sample at room temperature for 30 min.

−10 °C in 96% H_2SO_4. At room temperature, an IR ν(CO) band at 2194 cm^{-1} and the corresponding Raman band at 2196 cm^{-1} were observed (Figs. 15b, 15c), which are attributed to $Au(CO)^+$. The mutually exclusive IR and Raman ν(CO) bands at 2208 and 2247 cm^{-1} indicate a linear coordination ($D_{\infty h}$) for $Au(CO)_2^+$, the former due to the asymmetric CO stretch (Σ_u^+ normal mode) and the latter due to the symmetric CO stretch (Σ_g^+ normal mode). The linear structure has been observed in $[Au(CO)_2][Sb_2F_{11}]$[66] and $[Au(CO)_2]_2[SbF_6][Sb_2F_{11}]$.[68] $Au(CO)^+$ and $Au(CO)_2^+$ coexist in concentrated H_2SO_4 solution. $Au(CO)^+$ is stabler than $Au(CO)_2^+$; the unstable $Au(CO)_2^+$ readily releases one CO ligand to form $Au(CO)^+$ upon brief evacuation (Figs. 15b, 15c), while $Au(CO)^+$ remains unchanged even after a continuous evacuation over 24 hours (Scheme 3). A resonance at 171 ppm appears in the ^{13}C NMR spectrum at room temperature (Fig. 15d). After removing the ambient CO by evacuation, the solution gives a single peak at 164 ppm, which is due to $Au(CO)^+$. An equilibrium process between $Au(CO)^+$ and $Au(CO)_2^+$, which undergoes rapid CO exchange on the NMR time scale, would account for the single resonance. The chemical shift of $Au(CO)_2^+$ can be calculated to be 175 ppm by taking into consideration the CO/Au ratio.

In HSO_3F, the CO/Au stoichiometry reaches 2.0 at room temperature and remains at the same value at lower temperatures. An IR ν(CO) band at 2211 cm^{-1} (Fig. 16a) and a strongly polarized Raman band at 2249 cm^{-1} (Figs. 16d, 16e) were observed. These mutually exclusive IR and Raman ν(CO) bands indicate a linear coordination ($D_{\infty h}$) for $Au(CO)_2^+$, the former due to the asymmetric CO stretch (Σ_u^+ normal mode) and the latter due to the symmetric CO stretch (Σ_g^+ normal mode). $Au(CO)_2^+$ is stabler in HSO_3F than in concentrated H_2SO_4; it needs more than 14 h to remove one CO ligand to form $Au(CO)^+$, which shows an IR ν(CO) band at 2198 cm^{-1} (Fig. 16c). In the ^{13}C NMR spectrum at room temperature, a resonance at 174 ppm is observed for $Au(CO)_2^+$, in agreement with the previous observation.[66] After an evacuation for 14 h, the solution gives a single peak at 169 ppm due to a mixture of $Au(CO)^+$ and $Au(CO)_2^+$, which undergoes rapid CO exchange on the NMR time scale.

In magic acid, $HSO_3F{\cdot}SbF_5$ (1:1), the CO/Au stoichiometry reaches 2.0 at room temperature and remains at the same value at lower temperatures. An IR ν(CO) band at 2216 cm^{-1} (Fig. 17a) and a strongly polarized Raman band at 2252 cm^{-1} (Figs. 17d, 17e) were observed. As observed in HSO_3F, the mutually exclusive IR and Raman ν(CO) bands indicate a linear coordination ($D_{\infty h}$) for $Au(CO)_2^+$, the former due to the asymmetric CO stretch (Σ_u^+ normal mode) and the latter due to the symmetric CO stretch (Σ_g^+ normal mode). $Au(CO)_2^+$ is stabler in magic acid than in HSO_3F; it remains unchanged even after an evacuation of 13 h (Fig. 17c). In the ^{13}C NMR spectrum at room temperature, a resonance at 172 ppm is observed for $Au(CO)_2^+$.

All the IR and Raman ν(CO) values for $Au(CO)_n^+$ (n = 1, 2) are much higher than 2143 cm^{-1}, the value for free CO. The ^{13}C NMR chemical shifts shown by the gold(I) carbonyl cations are high-field-shifted from 184 ppm, the value for free

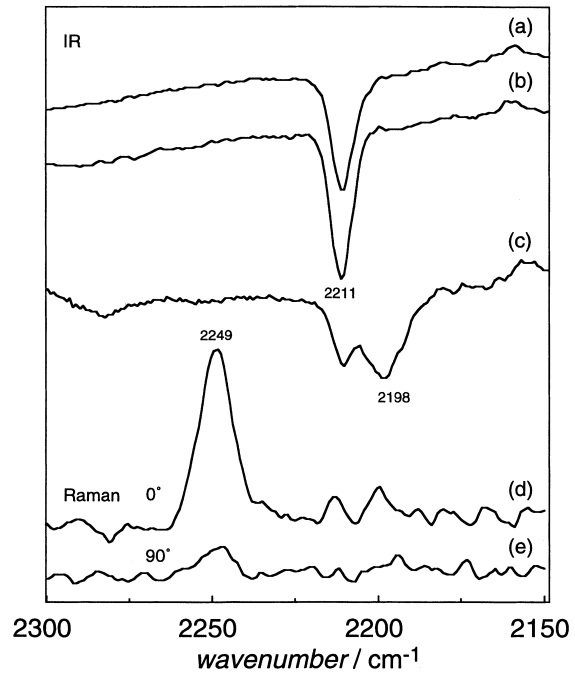

Fig. 16. IR spectra of gold(I) carbonyl cations in HSO_3F at (a) 25 °C and (b) −70 °C under atmospheric pressure of CO, and (c) after evacuating at room temperature for 14 h, and Raman spectra of the sample a with (d) 0° and (e) 90° polarization filters.

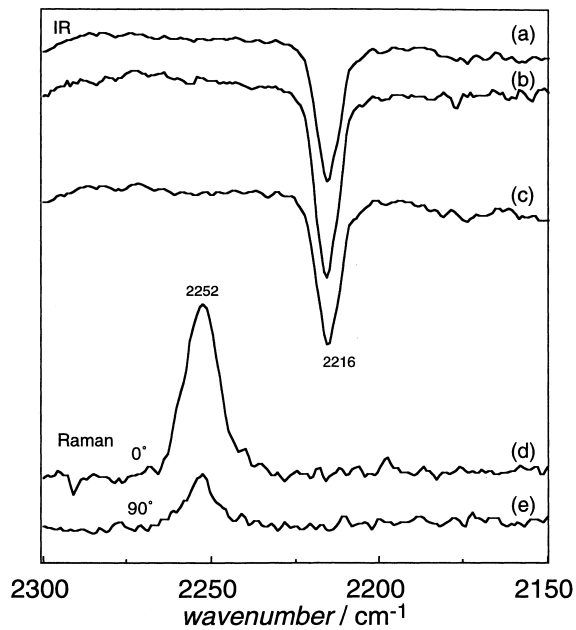

Fig. 17. IR spectra of gold(I) carbonyl cations in magic acid, $HSO_3F{\cdot}SbF_5$ (1:1), at (a) 25 °C and (b) −23 °C under atmospheric pressure of CO, and (c) after evacuating at room temperature for 13 h, and Raman spectra of the sample a with (d) 0° and (e) 90° polarization filters.

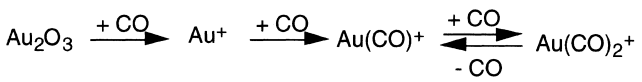

Scheme 3.

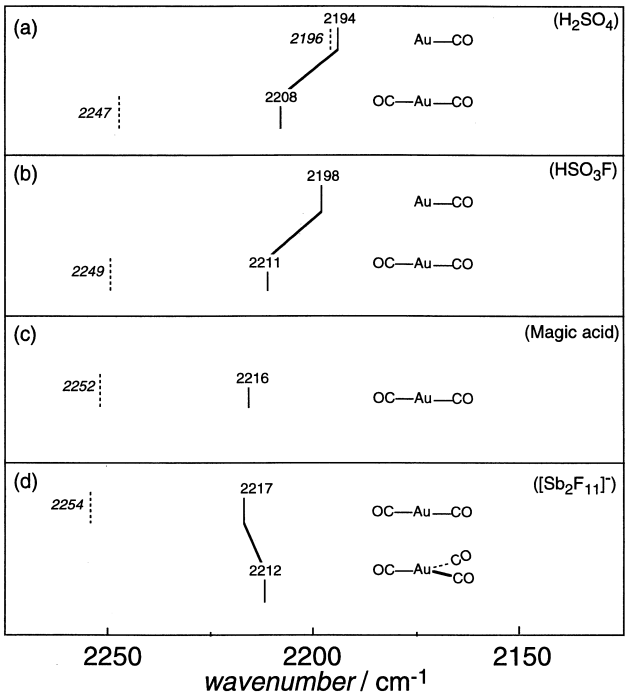

Fig. 18. Schematic representations of $Au(CO)_n^+$ (n = 1–3) species and corresponding CO vibrational frequencies in (a) 96% H_2SO_4, (b) HSO_3F, (c) magic acid, $HSO_3F{\cdot}SbF_5$ (1:1), and (d) the salt of $[Sb_2F_{11}]^-$. Full and dashed segments represent IR and Raman data, respectively.

CO. It is noted that, with increasing acidity of the solvent ν(CO) shifts to a higher frequency and $\delta(^{13}C)$ shifts to a higher field. The structure for $Au(CO)_2^+$ in all the three solvents is linear ($D_{\infty h}$) (Fig. 18).

(d) Comparison of Copper(I), Silver(I), and Gold(I) Carbonyls. It is very interesting that we could not observe $Au(CO)_3^+$ and $Au(CO)_4^+$ although $Cu(CO)_n^+$ (n = 1–4) and $Ag(CO)_n^+$ (n = 1–3) have been observed in strongly acidic solutions at atmospheric CO pressure, and the mono- and di- carbonyl cations of gold(I), $Au(CO)_n^+$ (n = 1, 2), are stabler than those of copper(I) and silver(I). These findings are in agreement with the properties of the metal-carbon bondings previously investigated by both experimental and theoretical methods. Armentrout and co-workers estimated metal-carbonyl bond energies for the gas phase complex ions $Cu(CO)_n^+$ and $Ag(CO)_n^+$ (n = 1–4): $(CO)_xCu^+CO$ bond energies at 0 K of 36, 41, 18, and 13 kcal/mol for x = 0, 1, 2, and 3, respectively; $(CO)_xAg^+CO$ bond energies at 0 K of 21, 26, 13, and 11 kcal/mol for x = 0, 1, 2, and 3, respectively.[63] Veldkamp and Frenking calculated (MP2 level of theory) $(CO)_xAg^+CO$ bond energies of 21, 27, and 12 kcal/mol for x = 0, 1, and 2, respectively; $(CO)_xAu^+CO$ bond energies of 45, 50, and 9 kcal/mol for x = 0, 1, and 2, respectively.[62] Zhou and Andrews reported calculations (B3LYP) of dissociation energies of $(CO)_xCu^+CO$ of 34.8, 35.6, 20.4, and 17.4 kcal/mol for x = 0, 1, 2, and 3, respectively.[47] These results predicted that the stability of $M(CO)^+$ and $M(CO)_2^+$ is in the order of Ag < Cu < Au, but the stability of $M(CO)_3^+$ is in the order of Au < Ag < Cu, in good agreement with the findings of the present work. The order for M–CO bond energies of $M(CO)_2^+$ has been explained by Strauss et al. using the s–d_σ energy gaps (corresponding to the lowest energy $d^9s^1 \leftarrow d^{10}$ electronic transition energies for the gas-phase M^+ cation; 2.7, 4.9, and 1.9 eV, respectively, for Cu, Ag, and Au) and d-subshell energy levels (corresponding to the second ionization energies; 20.3, 21.5, and 20.5 eV, respectively, for Cu, Ag, and Au).[67] For two-coordinate d^{10} metal complexes, sd_σ mixing results in a shift of electron density from the z axis (the metal-ligand axis) to the xy plane and decreases the σ-repulsion which allows for shorter, stronger metal-ligand σ-bonds. Among the three metals, Au(I) has the smallest s–d_σ energy gap, and therefore the Au–C σ-bonds in $Au(CO)_2^+$ are particularly strong. The reason why the third M–CO bond is so weak for gold may be that the d-orbital participation in M–C σ-bonding is so effective in $Au(CO)_2^+$ that bending the molecular framework is more destabilizing than for $Cu(CO)_2^+$ or $Ag(CO)_2^+$, as well observed for Au(I) which has a much reduced tendency to form three-coordinate complexes relative to Ag(I) and Cu(I).[67]

(e) Application of Copper(I), Silver(I) and Gold(I) Carbonyl Cations to Carbonylation of Olefins and Alcohols. The Koch reaction has been well-known for the synthesis of tertiary carboxylic acids from olefins and water, or alcohols, with carbon monoxide in strong acids (Scheme 4).[7,69] This reaction occurs at temperatures between −20 to 80 °C and at pressures up to 100 atm. Generally, H_2SO_4, H_3PO_4, HF and $BF_3{\cdot}H_2O$ are employed as catalysts and solvents.

The previous work by Souma et al. showed that copper(I) and silver(I) carbonyls in strong acids catalyze the carbonylation of olefins and alcohols to give tertiary carboxylic acids in high yields at room temperature and atmospheric pressure.[25–28] The polycarbonyl cations, $Cu(CO)_3^+$ and $Ag(CO)_2^+$, were assinged as the active species, respectively, in the carbonylation of olefins and alcohols in concentrated H_2SO_4.[54] The present work reveals that, when the copper(I) compounds are dissolved under CO atmosphere in concentrated H_2SO_4, $Cu(CO)_2^+$ is mainly formed with $Cu(CO)_3^+$ as the minor species, and when the silver(I) compounds are dissolved under CO atmosphere in concentrated H_2SO_4, only $Ag(CO)^+$ (no $Ag(CO)_2^+$) is formed. Therefore, $Cu(CO)_2^+$ (and $Cu(CO)_3^+$ as a minor species) and $Ag(CO)^+$ should be assigned as the active species, respectively, for the copper(I) and silver(I) carbonyl cation-catalyzed carbonylation of olefins and alcohols.

Xu and co-workers recently reported that the gold(I) carbonyl cations serve as an excellent catalyst, with which olefins readily react with CO to produce tertiary carboxylic acids in high yields at ambient CO pressure and temperature. $Au(CO)_2^+$ has been suggested to be the active species.[29] This is the first application of gold(I) carbonyls to organic syntheses; very few gold catalysts have been reported so far. Furthermore, it has been found that the palladium(I), rhodium(I) and platinum(I) carbonyl cations are excellent catalysts for the carbonylation of olefins and alcohols, for which $Pd_2(CO)_2^{2+}{}_{(solv)}$, $Rh(CO)_4^+$ and $[\{Pt(CO)_3\}_2]^{2+}$ are the active species, respec-

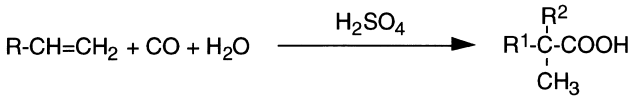

Scheme 4.

tively.[30–35]

A CO-carrier model was originally proposed for the reaction mechamism, in which the unstable metal polycarbonyl cations were considered to act merely as a *CO carrier*.[25] Recently, a reaction mechanism involving an olefin-metal-polycarbonyl intermediate has been proposed for the metal carbonyl cation-catalyzed carbonylation of olefins and alcohols in strong acids,[17,29] which is supported by the observations that $Pd_2(CO)_2^{2+}{}_{(solv)}$ and $[\{Pt(CO)_3\}_2]^{2+}$ are so stable that they cannot act as a mere CO carrier to transport CO from the gas phase but have catalytic activities comparable to those of copper(I), silver(I), gold(I), and rhodium(I) carbonyl catalysts.[30,35]

As described above, in concentrated H_2SO_4 only silver(I) monocarbonyl, $Ag(CO)^+$, is observed and therefore assigned as the active species for the carbonylation of olefins and alcohols, whereas polycarbonyl cations are observed for copper(I) and gold(I). These findings lead to a modified reaction mechanism in which an olefin-metal-monocarbonyl (eg., for Ag) or an olefin-metal-polycarbonyl (eg., for Cu or Au) may be an intermediate involved in the metal carbonyl cation-catalyzed carbonylation of olefins and alcohols in strong acids.

Conclusions

Detailed IR, Raman, and NMR spectroscopic characterization has been carried out on the group 11 metal carbonyl cations, $Cu(CO)_n^+$ (n = 1, 2, 3, 4), $Ag(CO)_n^+$ (n = 1, 2, 3), and $Au(CO)_n^+$ (n = 1, 2), over a wide range of temperature and in solvents of different acidities. Based on the spectroscopic data, the molecular structures of copper(I), silver(I) and gold(I) carbonyl cations have been determined. The $Cu(CO)^+$, the bent $Cu(CO)_2^+$ (C_{2v}) and the non-planar $Cu(CO)_3^+$ (C_{3v}) are formed in conc. H_2SO_4 and HSO_3F, whereas the bent $Cu(CO)_2^+$ (C_{2v}), the trigonal-planar $Cu(CO)_3^+$ (D_{3h}) and the tetrahedral $Cu(CO)_4^+$ (T_d) are formed in magic acid. The $Ag(CO)^+$, the linear $Ag(CO)_2^+$ ($D_{\infty h}$) and the trigonal-planar $Ag(CO)_3^+$ (D_{3h}) cations are formed in HSO_3F and magic acid, but only $Ag(CO)^+$ is formed in conc. H_2SO_4. The linear $Au(CO)_2^+$ and $Au(CO)^+$ are observed in all the acids, but no $Au(CO)_3^+$ and $Au(CO)_4^+$ were formed under atmospheric CO pressure.

This work reveals that, in concentrated H_2SO_4 under CO atmosphere at room temperature, $Cu(CO)_2^+$ is formed as the major species and $Cu(CO)_3^+$ as the minor species for Cu(I), and only $Ag(CO)^+$ (no $Ag(CO)_2^+$) is observed for Ag(I). The active species are therefore determined to be $Cu(CO)_2^+$ (and $Cu(CO)_3^+$ as a minor species) instead of the previously assigned $Cu(CO)_3^+$, $Ag(CO)^+$ instead of the previously assigned $Ag(CO)_2^+$, and $Au(CO)_2^+$ for the copper(I), silver(I) and gold(I) carbonyl cation-catalyzed carbonylation of olefins and alcohols. The reaction mechanism previously proposed for the metal carbonyl cation-catalyzed carbonylation of olefins and alcohols has been modified to involve an olefin-metal-monocarbonyl (e.g., for Ag) or an olefin-metal-polycarbonyl (e.g., for Cu or Au) intermediate.

References

1 F. A. Cotton, G. Wilkinson, C. A. Murillo, and M. Bochmann, "Advanced Inorganic Chemistry," 6th edn., Wiley, New York (1999).

2 P. Schützenberger, *C.R. Hebd. Seances Acad. Sci.*, **70**,1134 (1870).

3 P. Schützenberger, *C. R. Hebd. Seances Acad. Sci.*, **70**, 1287 (1870).

4 P. Schützenberger, *Bull. Soc. Chim. Fr.*, **14**, 97 (1870).

5 P. Schützenberger, *Bull. Soc. Chem. Fr.*, **10**, 188 (1868).

6 H. M. Colquhoun, D. J. Thompson, and M. V. Twigg, "Carbonylation: Direct Synthesis of Carbonyl Compounds," Plenum Press, New York (1991).

7 "New Syntheses with Carbon Monoxide," ed by J. Falbe, Springer-Verlag, Berlin, (1980).

8 E. I. Solomon, P. M. Jones, and J. A. May, *Chem. Rev.*, **93**, 2623 (1993).

9 A. Sen, *Acc. Chem. Res.*, **26**, 303 (1993).

10 K. C. Waugh, *Catal. Today*, **15**, 51 (1992).

11 M. A. Vannice, *Catal. Today*, **12**, 255 (1992).

12 G. Henrici-Olivé and S. Olivé, "The Chemistry of the Catalyzed Hydrogenation of Carbon Monoxide," Springer-Verlag, Berlin (1983).

13 F. Aubke and C. Wang, *Coord. Chem. Rev.*, **137**, 483 (1994).

14 L. Weber, *Angew. Chem.*, **106**, 1131 (1994), *Angew. Chem., Int. Ed. Engl.*, **33**, 1077 (1994).

15 S. H. Strauss, *Chemtracts-Inorg. Chem.*, **10**, 77 (1997).

16 H. Willner and F. Aubke, *Angew. Chem.*, **109**, 2506 (1997), *Angew. Chem., Int. Ed. Engl.*, **36**, 2402 (1997).

17 Q. Xu and Y. Souma, *Top. Catal.*, **6**, 17 (1998).

18 S. H. Strauss, *J. Chem. Soc. Dalton Trans.*, **2000**, 1.

19 A. J. Lupinetti, S. H. Strauss, and G. Frenking, *Progr. Inorg. Chem.*, **49**, 1 (2001).

20 H. Willner and F. Aubke, "Inorganic Chemistry Highlights" ed by G. Meyer, L. Wesemann, and D. Naumann, Wiley-VCH, Weinheim Germany (2002).

21 Q. Xu, *Coord. Chem. Rev.*, **231**, 83 (2002).

22 W. Manchot, J. König, and H. Gall, *Chem. Ber.*, **57**, 1157 (1924).

23 W. Manchot and J. König, *Chem. Ber.*, **60**, 2183 (1927).

24 Y. Souma, J. Iyoda, and H. Sano, *Inorg. Chem.*, **15**, 968 (1976).

25 Y. Souma, H. Sano, and J. Iyoda, *J. Org. Chem.*, **38**, 2016 (1973).

26 Y. Souma and H. Sano, *J. Org. Chem.*, **38**, 3633 (1973).

27 Y. Souma and H. Sano, *Bull. Chem. Soc. Jpn.*, **47**, 1717 (1974).

28 Y. Souma and H. Sano, *Bull. Chem. Soc. Jpn.*, **46**, 3237 (1973).

29 Q. Xu, Y. Imamura, M. Fujiwara, and Y. Souma, *J. Org. Chem.*, **62**, 1594 (1997).

30 Q. Xu, Y. Souma, J. Umezawa, M. Tanaka, and H. Nakatani, *J. Org. Chem.*, **64**, 6306 (1999).

31 Q. Xu, H. Nakatani, and Y. Souma, *J. Org. Chem.*, **65**, 1540 (2000).

32 Q. Xu, S. Inoue, Y. Souma, and H. Nakatani, *J. Organomet. Chem.*, **606**, 147 (2000).

33 Q. Xu, Y. Souma, B. T. Heaton, C. Jacob, and K. Kanamori, *Angew. Chem., Int. Ed.*, **39**, 208 (2000).

34 Q. Xu, B.T. Heaton, C. Jacob, K. Mogi, Y. Ichihashi, Y. Souma, K. Kanamori, and T. Eguchi, *J. Am. Chem. Soc.*, **122**, 6862 (2000).

35 Q. Xu, M. Fujiwara, M. Tanaka, and Y. Souma, *J. Org.*

Chem., **65**, 8105 (2000).
36 A. Neppel, J. P. Hickey, and I. S. Butler, *J. Raman Spectrosc*., **8**, 57 (1979).
37 F. Leblanc, *C. R. Acad. Sci. Paris*, **30**, 483 (1850).
38 M. Berthelot, *Ann. Chim. Phys*., **346**, 477 (1856).
39 O. H. Wagner, *Z. Anorg. Chem*., **196**, 364 (1931).
40 M. Håkansson and S. Jagner, *Inorg. Chem*., **29**, 5241 (1990).
41 M. Pasquali, C. Floriani, and A. A. Gaetani-Manfredotti, *Inorg. Chem*., **20**, 3382 (1981).
42 W. Backen and R. Vestin, *Acta Chem. Scand. A*, **33**, 85 (1979).
43 C. D. Desjardins, D.B. Edwards, and J. Passmore, *Can. J. Chem*., **57**, 2714 (1979).
44 K. Nakamoto, "Infrared and Raman Spectra of Inorganic and coordination Compounds," 5th edn., Wiley-Interscience, New York (1997).
45 R. Ettinger, P. Blume, A. Patterson, Jr., and P. C. Lauterbur, *J. Chem. Phys*., **33**, 1597 (1960).
46 J. J. Rack, J. D. Webb, and S. H. Strauss, *Inorg. Chem*., **35**, 277 (1996).
47 M. F. Zhou and L. Andrews, *J. Chem. Phys*., **111**, 4548 (1999).
48 A. Zecchina, S. Bordiga, M. Salvalaggio, G. Spoto, D. Scarano, and C. Lamberti, *J. Catal*., **173**, 540 (1998).
49 A. Zecchina, S. Bordiga, G. Turnes Palomino, D. Scarano, C. Lamberti, and M. Salvalaggio, *J. Phys. Chem. B*, **103**, 3833 (1999).
50 C. Lamberti, G. Turnes Palomino, S. Bordiga, G. Berlier, F. D'Acapito, and A. Zecchina, *Angew. Chem., Int. Ed*., **39**, 2138 (2000).
51 O. G. Polyakov, S. M. Ivanova, C. M. Gaudinski, S. M. Miller, O. P. Anderson, and S. H. Strauss, *Organometallics*, **18**, 3769 (1999).
52 S. M. Ivanova, S. V. Ivanov, S. M. Miller, O. P. Anderson, K. A. Solntsev, and S. H. Strauss, *Inorg. Chem*., **38**, 3756 (1999).
53 J. E. Ellis, *Adv. Organomet. Chem*., **31**, 1 (1990).
54 Y. Souma and H. Kawasaki, *Catal Today*, **36**, 91 (1997).
55 P. K. Hurlburt, O. P. Anderson, and S. H. Strauss, *J. Am. Chem. Soc*., **113**, 6277 (1991).
56 P. K. Hurlburt, J. J. Rack, S. F. Dec, O. P. Anderson, and S. H. Strauss, *Inorg. Chem*., **32**, 373 (1993).
57 P. K. Hurlburt, J. J. Rack, J. S. Luck, S. F. Dec, J. D. Webb, O. P. Anderson, and S. H. Strauss, *J. Am. Chem. Soc*., **116**, 10003 (1994).
58 J. J. Rack, B. Moasser, J. D. Gargulak, W. L. Gladfelter, H. D. Hochheimer, and S. H. Strauss, *J. Chem. Soc., Chem. Commun*., **1994**, 685.
59 E. Bernhardt, G. Henkel, H. Willner, G. Pawelke, and H. Bürger, *Chem. Eur. J*., **7**, 4696 (2001).
60 S. Bordiga, G. Turnes Palomino, D. Arduino, C. Lamberti, A. Zecchina, and C. Otero Areán, *J. Mol. Catal. A*, **146**, 97 (1999).
61 B. Liang and L. Andrews, *J. Phys. Chem. A*, **104**, 9156 (2000).
62 A. Veldkamp and G. Frenking, *Organometallics*, **12**, 4613 (1993).
63 F. Meyer, Y-M. Chen, and P. B. Armentrout, *J. Am. Chem. Soc*., **117**, 4071 (1995).
64 W. Manchot and H. Gall, *Chem. Ber*., **58**, 2175 (1925).
65 H. Willner and F. Aubke, *Inorg. Chem*., **29**, 2195 (1990).
66 H. Willner, J. Schaebs, G. Hwang, F. Mistry, R. Jones, J. Trotter, and F. Aubke, *J. Am. Chem. Soc*., **114**, 8972 (1992).
67 J. J. Rack and S. H. Strauss, *Catal. Today*, **36**, 99 (1997).
68 R. Küster and K. Seppelt, *Z. Anorg. Allg. Chem*., **626**, 236 (2000).
69 H. Koch, *Brennst. Chem*., **36**, 321 (1955).